ASIAN JOURNAL
ISSN: 0976-3376

Available Online at http://www.journalajst.com

ASIAN JOURNAL OF SCIENCE AND TECHNOLOGY

Asian Journal of Science and Technology
Vol. 4, Issue 07, pp.045-056, July, 2013

RESEARCH ARTICLE

HEAT TRANSFER AND FRICTION CHARACTERISTICS OF ARTIFICIALLY ROUGHENED SOLAR AIR HEATER DUCT: A REVIEW

[1]Pranab Kanti Roy and [2]Kisalaya Chakrabarti

[1]Department of Mechanical Engineering, Bengal Institute of Technology and Management, Santiniketan-731236, West Bengal, India
[2]Electronics and Communication Engineering, Bengal Institute of Technology and Management, Santiniketan-731236, West Bengal, India

ARTICLE INFO

Article History:
Received 09th April, 2013
Received in revised form
25th May, 2013
Accepted 19th June, 2013
Published online 19th July, 2013

Key words:
Solar air heater;
Artificial roughness,
Friction factor,
Hear transfer,
Correlation

ABSTRACT

The use of artificial roughness is an effective technique to enhance the rate of heat transfer by creating turbulence in a fully developed turbulent flow. Investigators reported number of roughness geometries on the heat transfer and friction characteristics of the artificially roughened solar air heater duct. In this paper an attempt has been made to review the different roughness arrangement and geometries to improve the heat transfer capability of solar air heater duct. The correlation of heat transfer and friction characteristics of 15 solar air heater ducts has been presented in Table1

INTRODUCTION

With the rapid rise in the population and the living standards, the world seems to flow over a major crisis, called energy crisis. The use of conventional sources of energy like coal, petroleum and natural gas are depleting at a very fast rate to fulfil the demand of incoming years. So there is a need to look for some other energy sources that could meet this growing demand. One such source is solar energy, which is cheap and available in abundance. Solar energy has been utilized in many ways some of its thermal applications are as follows. The simplest and the most efficient way to utilize solar energy are to convert it into thermal energy for heating applications as such the drying of agricultural products, seasoning of woods, space heating, curing of industrial products. The duct of a solar air heater that absorbs the incoming solar radiation, converting it into heat at the absorbing surface, and transfers this heat to a fluid (usually air or water) flowing through the collector as shown in Fig.1. The main demerit of the solar air heater is low thermal efficiency because of low heat transfer co-efficient of absorber plate. The heat transfer rate can be enhanced either by increasing the surface area or increasing the convective heat transfer coefficient by providing artificial roughness on the underside of the absorber plate. Under the method of artificial roughness, many experimental tests have been found in literature by various researchers.

***Corresponding author:** Pranab Kanti Roy
Department of Mechanical Engineering, Bengal Institute of Technology and Management Santiniketan-731236, West Bengal, India

Brij Bhusan and Ranjit Singh [1] presented a review on roughness geometry based on methodology of production of artificial roughness but there is need to categorized based primary and secondary flow along the absorber plate.

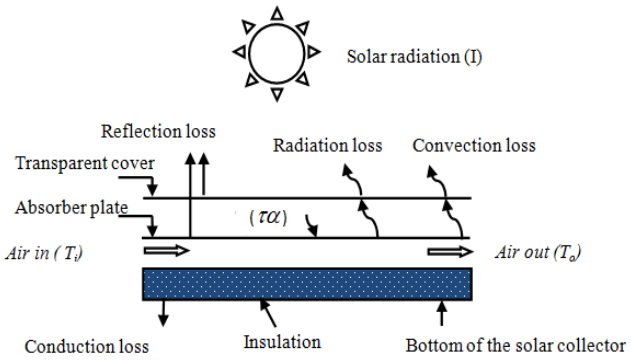

Fig. 1. A simple solar air heater duct

Thermal performances

The useful energy gain depends on heat transfer coefficient of air flowing through the duct which can be increased by artificial roughness of the absorber plate. It can be represented by non-dimensional number; Nusselt Number (Nu) Characteristics dimension (D) and thermal conductivity of air (k)

$$Nu = \frac{hD}{k}$$

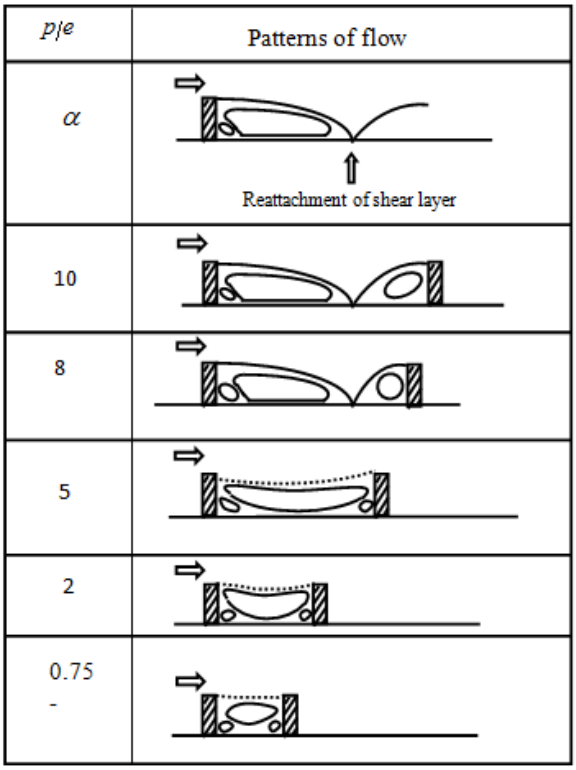

Fig. 2. Flow pattern depends on the relative roughness pitch [3,4]

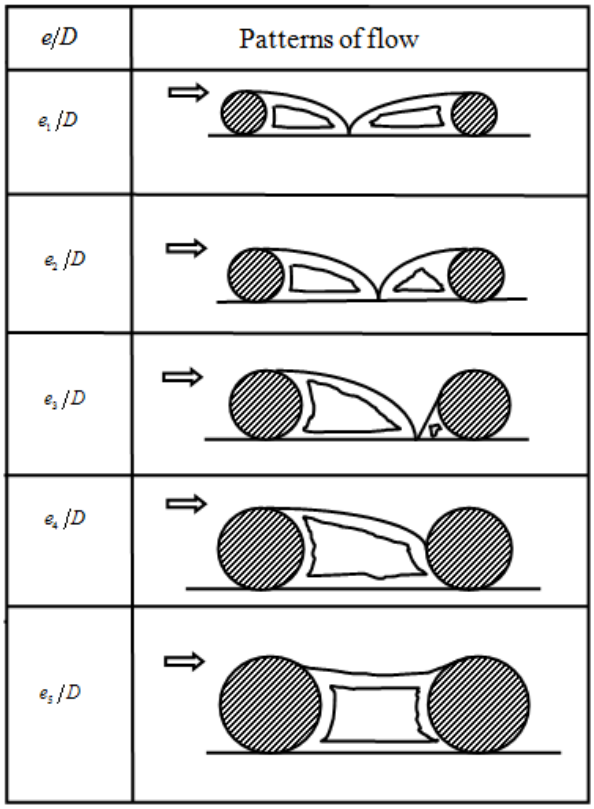

Fig. 3. Flow pattern depends on the relative roughness height [3,4]

Hydraulic performances

Hydraulic performances of a solar air heater concerns with the pressure drop (p/e) in the duct. The pressure drops is because of energy consumption by the fan to propel the air through the duct. The pressure drop can be represented by non-dimensional number in terms of friction factor (f) reported by Frank and Mark [2]

$$f = \frac{(\Delta p)D}{2\rho LV^2}$$

Thermo-hydraulic performances

The study of the heat transfer and friction characteristics of the roughened duct reveals that the enhancement in heat transfer rate also simultaneously increases in the friction factor. Therefore, it is essential to determine the geometry that will result maximum enhancement in heat transfer with minimum consumption of friction power. Lewis [23] proposed the thermo hydraulic performance of a roughened duct compared to that of smooth duct for the same pumping power requirement as defined as

$$\eta = \frac{Nu_r}{Nu_s} \Big/ \left(\frac{f_r}{f_s}\right)^{\frac{1}{3}}$$

Smooth surface

The velocity distribution of smooth surface can be expressed considering the law of wall [28]

$u^+ = y^+$ For laminar sub layer $y^+ \le 5$

$u^+ = 5\ln y^+ + 3.5$ For buffer sub layer $5 \le y^+ \le 30$

$u^+ = 5\ln y^+ + 3.5$ For turbulent layer $y^+ \ge 30$

Rough surface

For the rough surface considering the flow and roughness height i.e. a new combine hydrodynamic parameter is defined called roughness Reynolds number [3]. It is expressed as

$$e^+ = \frac{e}{D}\frac{\sqrt{f}}{\sqrt{2}}\mathrm{Re}$$

When $e^+ \le 5$, the friction factor is same for rough and smooth surface because the projections lie entirely within the laminar sub layer and flow is hydra dynamically smooth.

When $5 \le e^+ \le 70$, the protrusions of the roughness elements are same order of magnitude as the thickness of the laminar sub layer and the flow if transitionally rough.

And when $e^+ \ge 70$, the protrusion of the roughness elements extends beyond the laminar sub layer and flow is fully rough. The momentum transfer function can be written as

$$R(e^+) = \sqrt{\frac{2}{f}} + 2.5\ell n\left(\frac{2e}{D}\right) + 3.75$$

Heat transfer with flow separation and reattachment

The repeated circular and square rib surface as shown in Fig.3 and Fig. 4 respectively. The roughness geometry of boundary layer square rib surface for flow separation and reattachment is as shown in Fig 5. The separation occurs at the tip of the rib, which lead to the formation of a free shear layer and finally reattaches at about 6-8 times the rib height, downstream from the separation point as shown in Fig 2. The reverse flow boundary layer originates from the reattachment point and grows in thickness in the opposite direction of upstream region of the next consecutive rib. The boundary layer tends towards redevelopment downstream from the reattachment point. The wall shear stress is zero at the reattachment point and increases in the reverse flow and from reattachment region, however the direction of shear stress is opposite in that region.

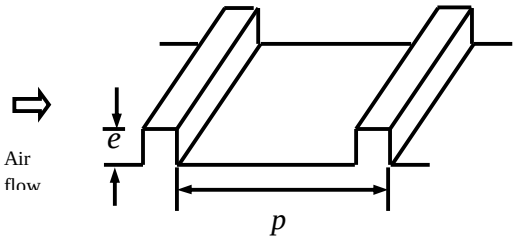

Fig. 4. Flow with transverse square ribs [24]

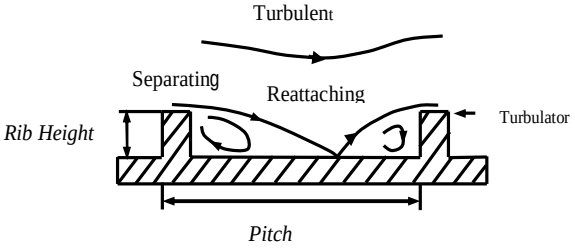

Fig. 5. Ribs with flow separation and reattachment [24]

When shear stress is zero at the reattachment point the friction factor becomes independent of Reynolds number and vortices of various sizes of the turbulent zone can penetrate into the laminar sub layer and reached the surface of the boundary. Reattachment does not occur for roughness pitch (p/e) less than about 8. Measurement of the local heat transfer coefficient downstream from the ribs [3] show that a maximum heat transfer coefficients occur in the area of reattachment point. The local heat transfer coefficients in the separated flow region are larger than those of an undisturbed boundary layer, but this is not true for laminar flow downstream from a rib.

Transverse continuous rib

These types of ribs are produced either by fixing circular wire or by maching the underside of the absorber plate of solar air heater duct. These types of ribs are placed at right angle to the direction of mainstream flow of absorber plate.

Prasad and Saini [4] investigated the effect of roughness height (e/D) and roughness pitch (p/e) on the heat transfer and fluid flow characteristics of solar air heater duct under the fully developed turbulent flow as shown in fig 9. The range of Reynolds number (Re) from 5000-50000, roughness height (e/D) from 0.02 -0.033, roughness pitch (p/e) 10, 15, 20 were selected for the experiment. It has been observed that the increase in relative roughness pitch beyond 10 and decrease in relative roughness pitch below 8, the reattachment of free shear layer does not occur at all. Again increase in relative roughness height results absence of reattachment of free shear layer. It has been reported that the optimum thermo hydraulic performance could be achieved at e^+ of 24. The maximum heat transfer coefficient and friction of the roughened surface over a smooth surface are 2.38 and 4.25 times respectively corresponding to relative roughness pitch (p/e) 10 and relative roughness height (e/D) 0.033.

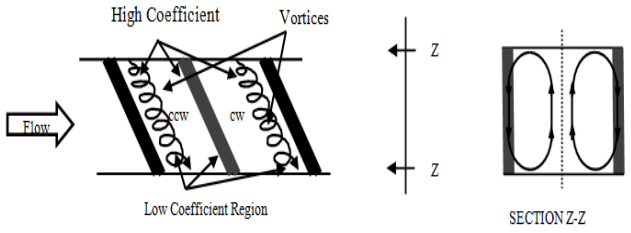

Fig. 6. Circulation for inclined rib [30]

Verma and Prasad [5] reported an outdoor experimental investigation for the thermohydraulic performance of the transverse circular wire ribs of solar air heater duct. The range of Reynolds number from 5000-20000, relative roughness pitch from 10-40, relative roughness pitch 0.01-0.03 were selected. The corresponding range of thermohydraulic roughness Reynolds number (e^+) 8-42.It has been observed that if the thickness of roughness Reynolds number lies above the laminar sublayer that gives the maximum heat transfer with minimum pressure drop. They evaluated the optimum value for transverse circular ribs corresponding to $e^+_{opts} = 24$ be equal to about 71%.

Wedge shape ribs

Williams *et al*. [29] reported the heat transfer and fluid flow characteristics of transverse wedge shape ribs better than the any other transverse ribs. In case of square and chamfered ribs as shown in Fig. 23 the eddies are generated on both sides of the ribs which reduce the heat transfer rate. But in case of wedge ribs, there is a relatively lesser chance of forming such stagnant eddies behind the ribs and this leads to a substantially larger enhancement of heat transfer rate. Bhagoria *et al*. [11] experimentally studied the heat transfer and fluid flow characteristics of transverse wedge shape ribs of a rectangular solar air heater duct as shown in Fig. 11. The range of parameter selected were, Reynolds number from 3000-18000, relative roughness pitch (p/e) from $60.17\Phi^{-1.0264}$ to 12.12, the rib wedge angle (Φ) 8^o to 15^o, relative roughness height range of 0.015-0.033. It has been observed that the maximum heat transfer occurs at a wedge angle of about 10 while on either side of this wedge angle, Nusselt number decreases. The

friction factor increases as the wedge angle increases. Authors reported at relative roughness pitch (p/e) of 12.12 and relative roughness height (e/D) of 0.033, the maximum of Nusselt number occurs nearly for a wedge angle of 10^o The heat transfer coefficient and friction factor for wedge roughened surface over smooth surface is 2.4 and 5.3 times respectively and it is at the relative roughness pitch (p/e) of about 7.57 and produce more turbulence at the reattachment point

Chamfered ribs

Karwa *et al*. [10] performed an experimental investigation of heat transfer and friction characteristics for a rectangular duct having aspect ratio (W/H) 4.8, 6.1, 7.8, 9.66 and 12.0 roughened with repeated chamfered ribs as shown in Fig 10. The geometric and operating parameter for this experiment were Reynolds number (Re) from 3000 to 20000, relative roughness height (e/D) 0.014 to 0.038, relative roughness pitch (p/e) 4.6 to 8.5, chamfer angle (Φ) from -15^o to $+18^o$.It is observed that the heat transfer function increases with the increase in aspect ratio from 4.65 to 9.66 and the roughness function decreases with the increase in the aspect ratio from 4.65 to 7.75. The highest value of heat transfer and friction factor occurs at the chamfer angle (Φ) of 15^o

Chamfered rib-groove turbulators

Layek *et al*. [13] carried out an experimental investigation to study the heat transfer and friction characteristics of repeated integral transverse chamfered rib with groove combination of a roughened absorber plate as shown in Fig.16 The parameters under investigation were Reynolds number range of 3000–21,000, relative roughness pitch (p/e) of 4.5–10, chamfer angle (Φ) 5^o–30^o, relative groove position (g/p) of 0.3–0.6 and relative roughness height of 0.022–0.04.

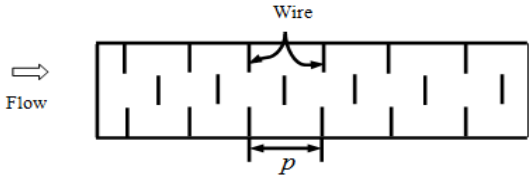

Fig. 8. Discrete circular ribs [8]

It has been observed that Nusselt number ratio enhancement achieved varies from 2.0 to 2.6 for entire data collected from this investigation revealed that the chamfered rib-groove roughness with relative roughness pitch (p/e) of 6, groove position to pitch ratio (g/p) of 0.4, chamfered angle (Φ) 18 and relative roughness height (e/D) 0.04 yields the maximum Nusselt number enhancement in the order of 3.24

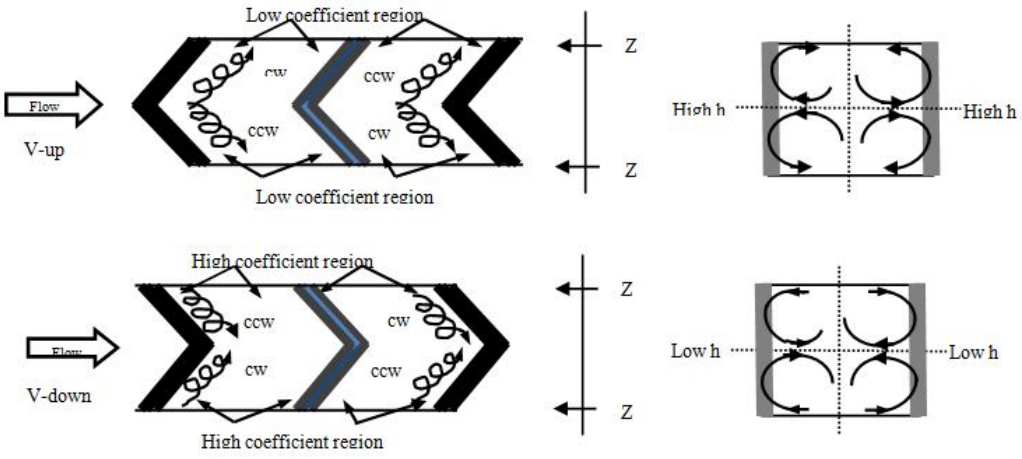

Fig. 7. Circulation of V-Shape rib [30]

Rib-groove turbulators

Jaurker *et al*. [12] experimentally studied the heat transfer and friction characteristics for repeated transverse rib groove combination on the absorber plate of the solar air heater duct as shown in Fig. 17. The geometrical parameter of the roughened absorber plate has a value of relative roughness pitch (p/e) 4.5 to 10.0; relative roughness height (e/D) 0.0181 to 0.363 and relative groove position (g/e) 0.3 to 0.7.The Reynolds number has value from 3000 to 21,000.It has been observed that Nusselt number is maximum at value of relative roughness pitch 6.0 and relative groove of 0.4 and its value is 2.75 times of smooth duct and 1.57 times of ribbed duct whereas for ribbed duct with similar rib height and rib spacing provides the Nusselt number values of the order of 1.7 times of the smooth duct for the range of experimentation.

times that of smooth surface at Reynolds number 21000 while friction factor is of 3.78 times of smooth surface.

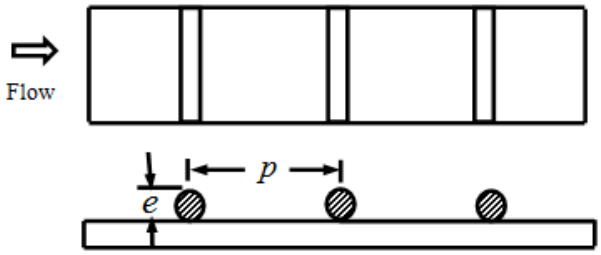

Fig. 9. Transverse continuous circular wire ribs [4]

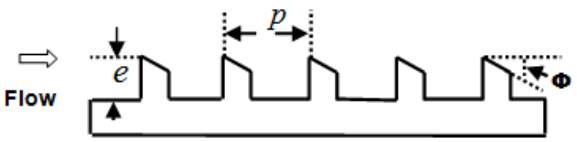

Fig. 10 Absorber plate with chamfered ribs [10]

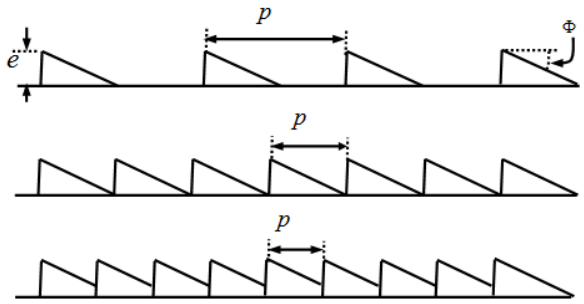

Fig. 11. Absorber plate with wedge ribs [11]

Wedge rib-groove turbulators

Pawar CB *et al*. [14] carried out an experimental investigation on the heat transfer and friction characteristics of solar air heater duct with wedge groove combination as shown in Fig. 15. The parameters under investigation were the wedge angle (Φ) varied from 10^o to 25^o for relative roughness height (e/D) maintained as 0.033 and relative roughness pitch (p/e) was kept 8 and range of Reynolds number 3000-20000. The relative groove position (g/p) was kept constant during the experiment. Authors reported that maximum heat transfer is 1.5-3 times of the smooth duct and friction factor 2 to 3 times of the smooth duct corresponding to wedge angle 15^o.

Inclined continuous ribs

It is found that in case of 90^o transverse rib there are two stagnant vortices immediately upstream and downstream of the rib with respect to the main flow which raises the local fluid temperature in the vortices and wall temperature near the rib resulting low heat transfer coefficient. By inclining the rib on the absorber plate these two stagnant eddies moves along the ribs and subsequently joins the main flow by creating a rotating secondary flow, which brings the lower duct fluid temperature near the angled ribs leading edge, increases the local heat transfer coefficient at constant heat flux as shown in Fig 6. Gupta *et al*. [6] investigated the effect of inclination angle of a circular wire ribs with respect to the direction of flow on the thermo hydraulic as well as thermal performance of a roughened rectangular solar air heater duct.

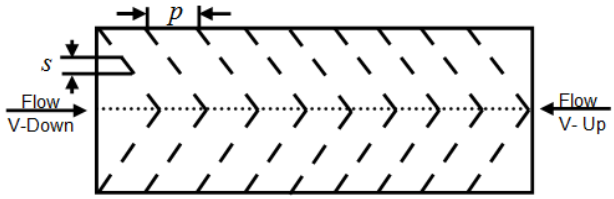

Fig. 12. Discrete V-shape ribs [9]

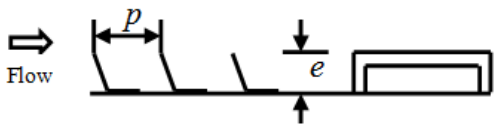

Fig. 13. Inverted U-shape Turbulator [15]

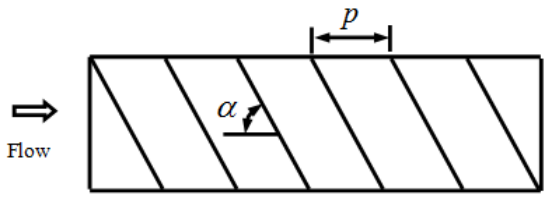

Fig. 14. Inclined circular wire ribs [6]

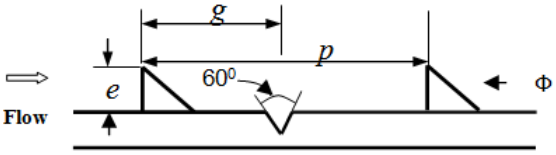

Fig.15. wedge ribs with groove [14]

The type and arrangement of the absorber plate is shown in Fig 14. They reported the maximum heat transfer enhancement occur at an angle of attack 60^0. Also they evaluated the optimum thermo hydraulic performance i.e. maximum heat transfer with minimum pressure drop corresponding to roughness height of 0.033.

V-shape ribs (Adjoin of two inclined ribs)

The heat transfer can be enhanced by the creation of secondary flow which is possible by angling the ribs due to the creation vortices as shown in fig.7. This creates a region of higher heat transfer near the leading edge of the rib and a region of low heat transfer near the trailing edge of the ribs. Therefore joining of two angled ribs in the form of V-shape results two leading edge and one trailing edge as in case of V shape ribs. The V-shape ribs having one leading edge and two trailing edge are known as V-up ribs. Hence in this way the V-down ribs approximately having two higher heat transfer region and one lower heat transfer region and V-up ribs having one higher heat transfer region and two lower heat transfer region. Momim *et al* [7] carried out an experimental investigation of the effect the geometrical parameters of V-shape ribs as shown in fig.22. Investigation covers a range of Reynolds number 2500-18000, relative roughness height of 0.02-0.034 and angle of attack of flow of 30^0-90^0 for a fixed relative roughness pitch of 10. It was observed that the rate of increase of increase of Nusselt number with an increase of friction factor; this appears due to the fact that at relatively higher values of relative roughness height, the reattachment of free shear layer might not occur and the rate of heat transfer enhancement will not be proportional to that of friction factor. It was found that for relative roughness height of 0.034 and for angle of attack 60^0,.the V-shape ribs enhance the values of Nusselt number by 1.14 and 2.30 times over the inclined ribs and smooth plate at Reynolds number 17034.It means that the V-shape ribs has definite advantage over the inclined ribs under same operating condition.

W-shape ribs (Combination of four inclined ribs)

The enhancement of the wall heat transfer by the use of V-shape ribs is based on the observation of the creation of secondary flow cell due to inclination of the rib resulting in a region of high heat transfer near the leading edge. When two angled ribs are joined together in the form of V-shape form two leading edge and one trailing edge, and thus develops a region of almost double heat transfer rate. Therefore W-shape roughness geometry gives better performance than the V-shape roughness geometry since its leading is more than trailing edge.

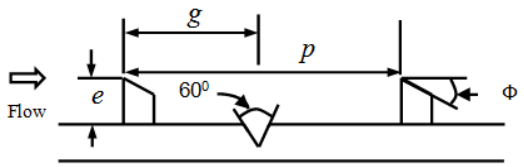

Fig. 16. Chamfered ribs with groove [13]

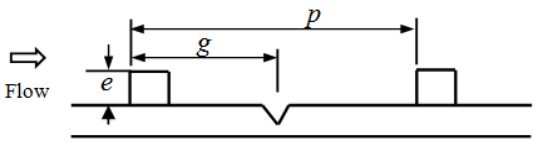

Fig. 17. Square rib with groove [12]

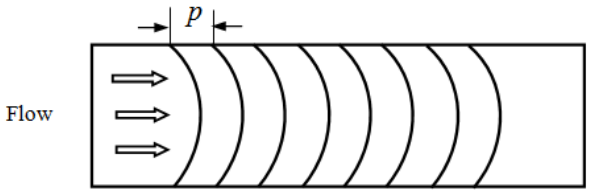

Fig. 18. Arc shape ribs roughened surface [16]

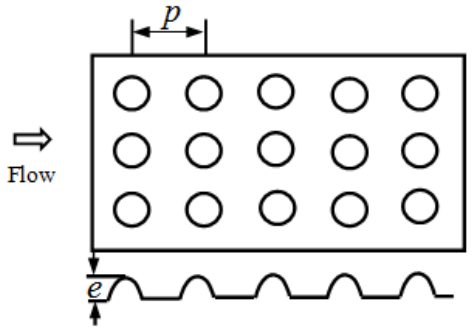

Fig. 19. Dimple shape roughness wit protrusions [18]

Kumar *et al*. [20] investigated the heat transfer and friction characteristics of W-shape discrete artificially roughened solar heater air heater duct as shown in Fig.24. The parameter under investigation was, Reynolds number (Re) 3000 to 15000, relative roughness height (e/D) in the range 0.0168 to 0.0338, relative roughness pitch (p/e) 10, and the angle of attack (α) in the range of 30° to 75°.They reported maximum enhancement in heat transfer and friction factor has been found to be 2.16 and 2.75 times that of smooth duct for an angle of attack of 60°.

W-up and W-down ribs

Lanjewar *et al* [21] reported the heat transfer and friction characteristics of solar air heater duct with W-shape ribs pointing downstream and upstream as shown in Fig.20a and Fig. 20b respectively. The duct width to height ratio(W/H) of 8, relative roughness pitch (p/e) 10, relative roughness height (e/D) 0.03375, angle of attack (α) of ribs in W-pattern is 45^0 and Reynolds number from 2300-14000.The enhancement of heat transfer by providing W-shape ribs is 2.39 for W-down and 2.21 W-up than the smooth duct. Author reported that W-down ribs give better thermo-hydraulic performance than W-up and V-ribs. The maximum thermo hydraulic performance for W-down ribs is 1.98 while it is 1.81 for W-up ribs in the range of parameters investigated.

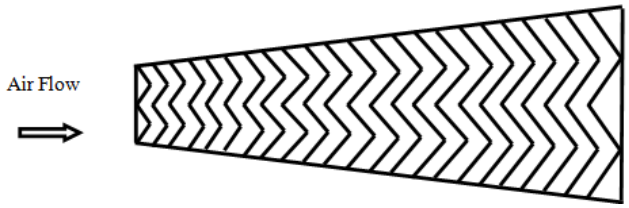

Fig. 20a. W-down roughness [21]

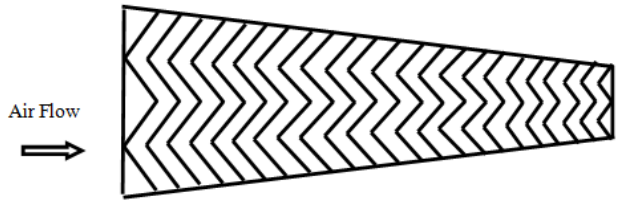

Fig. 20b. W-up roughness geometry [21]

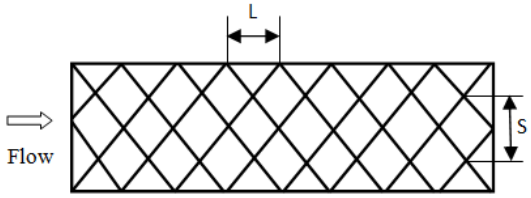

Fig. 21. Expanded metal mesh roughness [17]

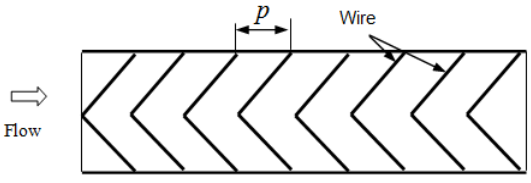

Fig. 22. V-shape circular wire ribs [7]

V-shaped staggered discrete ribs

Muluwork *et al*. [9] investigated the thermal performance staggered discrete V-shape ribs as shown in Fig.12 with apex facing up and down. They studied the effect of relative length ratio (B/S), relative roughness segment ratio (S'/S), and angle of attack (α) on the heat transfer and friction factor. The

relative roughness length ratio is considered as geometric parameter to compare three different configuration of the roughness element with constant roughness height (e/D) of 0.02. Stanton number increases with the increase of relative roughness length ratio. The heat transfer coefficient of V-down discrete ribs is higher than V-up and transverse discrete rib roughened solar air heater duct. The Stanton number for V-down discrete ribs is 1.32-2.47 for the range of parameter under investigation.

Metal grit ribs

Karmare and Tikekar [22] investigated for the range of Reynolds Number (Re) 4000 to 17000, the effect of grit geometry i.e. the relative roughness height of grid (e/D) from 0.035 to 0.044, the relative roughness pitch of grid (p/e) from 12.5 to 36, the relative length of metal grit (l/s) 1 to 1.72 as shown in Fig. 28. They reported the optimum them hydraulic performance corresponding to the values: $(l/s = 1.72)$, $(e/D) = 0.044$, $(p/e) = 12.5$

Multiple V-ribs

Hans *et al*.[26] reported the heat transfer and fluid flow characteristics of solar air heater duct with multiple V-shape artificial roughness as shown in Fig. 27 The range of parameter, Reynolds number from 2000-20,000, relative roughness height (e/D) of 0.019-0.043, relative roughness pitch (p/e) of 6-12,angle of attack (α) of 30°-75° and relative roughness width range (w/W) 1-10.The maximum enhancement in Nusselt number and friction factor due to presence of multiple V-ribs is 6 and 5times respectively in comparison to the smooth duct respectively.

Transverse broken ribs

Airflow over 90^0 transverse ribs on a rib roughened wall separates at the top edges of the ribs. The flow reattaches in a region downstream of the ribs. A boundary layer and reverse flow boundary layer in the region of reattachment and grow in thickness in opposite directions. Recirculation zone can be found adjacent to the upstream face, the downstream face and sometimes in some situations on the top face of the ribs. In case of air flow of 90° transverse broken ribs, the separation occurs not only on the top edge of the ribs but also at the end of the ribs, this secondary flow may also produce additional turbulence in the nearby reattachment zone Sahu and Bhagoria [8] reported the effect of transverse broken ribs affixed on the underside of solar air heater duct as shown in Fig. 8. The roughened wall has roughness with pitch ranging from 10-30mm, height of the rib of 1.5mm and duct aspect ratio of 8. Reynolds number ranging from 3000-12000.The heat transfer coefficient of the rough surface is 1.25-1.40 times of smooth surface and maximum efficiency is 83.5% can be obtained.

Inclined ribs with gaps

The introduction of gap in the inclined ribs results a release secondary flow which accelerate the retarded main flow. Because of this acceleration of main flow, the viscous boundary layer is broken and reattached with the surface and leads to higher heat transfer rate. But location of gap of the inclined ribs that means release of more secondary flow to energizing the retarded flow effect the heat transfer rates as shown in Fig 25. Again the gap width of the ribs that means the flow velocities must be sufficient enough to accelerate the main flow which ultimately increases the heat transfer rate.

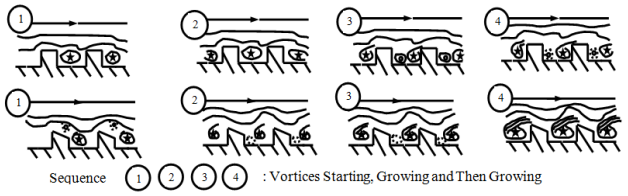

Fig. 23. Flow Pattern of square ribs and chamfered ribs [29]

Aharwal *et al*. [31] experimentally studied the heat transfer and friction characteristics of a rectangular duct roughed with repeated rib with a gap, and at an inclination with respect to the flow direction as shown in Fig.25. The roughened duct had an aspect ratio of 5.84, the relative gap position and relative gap width has been varied from 0.16 to 0.5 and 0.5 to 2.0 respectively. The range of Reynolds number from 3000 to 18000 with the relative roughness pitch range of 4-10; relative roughness height range of 0.018-0.037; and angle of attack range of 30-90°. The study shows that a maximum enhancement in Nusselt number of 2.83 times, in friction factor 2.89 times and in thermo hydraulic performance of 1.97 times compared to smooth duct in the range of operating parameters.

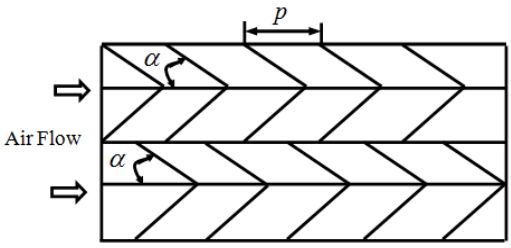

Fig. 24. Discrete W-shape roughness [20]

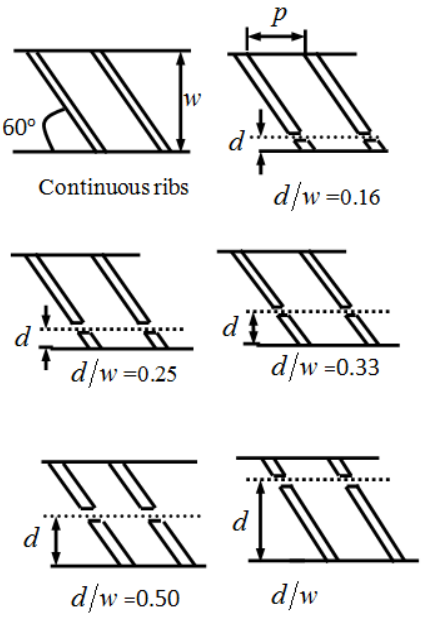

Fig. 25. discontinuous inclined ribs [31]

Table 1

Geometry of surface/ Author	Range of parameters	Correlation	
		Heat Transfer	Friction factor
Smooth surface Dittus-Boilter and Blasius		$h_r = (k/d) \times \mathrm{Re}^{0.8} \times \mathrm{Pr}^{0.4}$	$f_r = 0.85 \times \mathrm{Re}^{-0.25}$
Transverse protrusion wire Prasad and Saini[4]	$e/D: 0.020 - 0.033$ $p/e: 10 - 20$ $\mathrm{Re}: 50000 - 50{,}0000$	$St = \dfrac{f/2}{1+\sqrt{f/2}\left\{4.5\left(e^{+}\right)^{0.28}\mathrm{Pr}^{0.57} - 0.95(p/e)^{0.55}\right\}}$	$fr = \dfrac{2}{\left[0.95(p/e)^{0.53} + 2.5\ln(D/2e - 3.75)\right]^2}$
Transverse protrusion wire Verma and Prasad[5]	$e/D: 0.010 - 0.030$ $p/e: 10 - 40$ $\mathrm{Re}: 5000 - 20.000$ $e^{+}: 8 - 42$	$0.08596(p/e)^{0.054}(e/D)^{0.072}(\mathrm{Re})^{0.723}\ for, e^{+} \le 24$ $Nu = 0.02954(p/e)^{-0.016}(e/D)^{0.021}\mathrm{Re}^{0.802}\ for, e^{+} > 24$	$f = 0.245(p/e)^{-0.206}(e/D)^{0.243}\mathrm{Re}^{-1.25}$
Transverse protrusion wire Gupta et al.[27]	$e/D: 0.018 - 0.052$ $\mathrm{Re}: 3000 - 18{,}000$	$Nu = 0.000824\ (e/D)^{-0.178}(W/H)^{0.284}(\mathrm{Re})^{1.062}$ $e^{+} \le 35$ $Nu = 0.00307\ (e/D)^{-0.469}(W/H)^{0.245}(\mathrm{Re})^{($ $e^{+} \ge 35$	$f = 0.06412\ (e/D)^{0.019}$ $\times (W/H)^{0.0237}(\mathrm{Re})^{-0.185}$
Inclined wire ribs Gupta et al.[6]	$e/D: 0.020 - 0.053$ $p/e: 10 - 20$ $\alpha: 30^{o} - 60^{0}$ $\mathrm{Re}: 5000 - 30{,}000$	$Nu = 0.000824\ (e/D)^{-0.178}(W/H)^{0.284}(\mathrm{Re})^{1.062}$ $\exp\left[-0.04(1-\alpha/60)^2\right](k/D)e \le 35$ $Nu = 0.000824\ (e/D)^{-0.469}(W/H)^{0.245}(\mathrm{Re})^{0.812}$ $\exp\left[-0.0475(1-\alpha/60)^2\right](k/D)e \ge 35$	$f = 0.06412\ (e/D)^{0.019}$ $\times (W/H)^{0.0237}(\mathrm{Re})^{-0.185}$ $\exp\left[-0.0993\ (1-\alpha/70)^2\right]$
V-shape continuous ribs Momim et al.[7]	$e/D: 0.020 - 0.053$ $p/e: 10$ $\alpha: 30^{o} - 60^{o}$ $\mathrm{Re} = 2500 - 18{,}000$	$Nu_r = 0.067\ \mathrm{Re}^{0.888}(e/D)^{0.424}(\alpha/60)^{-0.077} \times$ $\exp\left[-0.0782\ \{\ln(\alpha/60)\}^2\right]$	$f_r = 6.266\mathrm{Re}^{-0.425}(e/D)^{0.565}(\alpha/60)^{-0.093}$ $\times\exp\left[-0.719\{\ln(\alpha/60)^2\}\right]$
V-shape staggered discrete ribs Muluwork et al.[9]	$e/D: 0.020$ $\alpha: 60^{o}$ $B/S: 3 - 9$ $\mathrm{Re}: 2000 - 15{,}000$	$Nu_r = 0.00534\ \mathrm{Re}^{1.2991}(p/s)^{1.3496}$	$f_r = 0.7117\ \mathrm{Re}^{-2.991}(p/S)^{0.0636}$
Chamfered rib Karwa et al.[10]	$(p/e): 4.5 - 40$ $\mathrm{Re}: 2500 - 18{,}000$ $W/H: 4.8, 6.1, 7.8, 9.66$ $and, 12$	$g = 103.77\ e^{-0.006\Phi}(W/H)^{0.5}(p/e)^{-2.56}$ $\times \exp\left[0.7343\ \{\ln(p/e)\}^2\right](e^{+})^{-0.31}$ $for, 7 \le e^{+} \le 20$ $g = 32.26\ (W/H)^{0.5}(p/e)^{-2.56}$ $\times \exp\left[0.7343\ \{\ln(p/e)\}^2\right](e^{+})^{-0.08}$ $for, 20 < e^{+} < 60$	$R = 1.66\, e^{-0.0078\Phi}(W/H)^{-0.4}(p/e)^{2.695}$ $\times \exp\left[-0.762\ \{\ln(p/e)\}^2\right](e^{+})^{-0.075}$ $for, 5 \le e^{+} \le 20$ $R = 1.32\, e^{-0.0078\Phi}(W/H)^{-0.4}(p/e)^{2.695}$ $\times \exp\left[-0.762\ \{\ln(p/e)\}^2\right]$ $for, 20 \le e^{+} < 60$
Wedge shape rib Bhagoria et al.[11]	$e/D: 0.015 - 0.033$ $p/e: 60.17\phi^{-1.0264} < p/e < 12.12$	$Nr = 1.89 \times 10^{-4}(\mathrm{Re})^{1.21}$ $\times (e/D)^{0.426}(p/e)^{2.94}$ $\times \left[\exp\left(-0.71\ \{\ell n(p/e)\}^2\right)\right](\phi/10)^{-0.018}$ $\times \exp\left[-1.5\ \{\ln(\Phi/10)\}^2\right]$	$f_r = 12.44\ \mathrm{Re}^{-0.18}(e/D)^{0.99}$ $(p/e)^{-0.52}(\Phi/10)^{0.49}$
Square groove rib Juarker et al.[12]	$\mathrm{Re}: 3000 - 21{,}000$ $e/D = 0.0181 - 0.0363$ $p/e = 4.5 - 10.0$ $g/P = 0.3 - 0.7$	$Nu = 0.002062\ \mathrm{Re}^{0.936}\left(\frac{e}{D}\right)^{0.349}\left(\frac{p}{e}\right)^{3.318}$ $\times \exp\left[-0.868\left\{\ln\left(\frac{p}{e}\right)\right\}^2\right]\left(\frac{g}{p}\right)^{1.108}$ $\times \exp\left[2.486\left\{\ln\left(\frac{g}{p}\right)\right\}^2 + 1.406\left\{\ln\frac{g}{p}\right\}^3\right]$	$f = 0.001227(\mathrm{Re})^{-0.199}\left(\frac{e}{D}\right)^{0.585}\left(\frac{p}{e}\right)^{7.19}\left(\frac{g}{p}\right)^{0.645}$ $\times \exp\left(-1.854\left\{\ln\frac{p}{e}\right\}^2\right)$ $\times \exp\left(1.513\left\{\ln\left(\frac{g}{p}\right)\right\}^2 + 0.8662\left\{\ln\left(\frac{g}{p}\right)\right\}^3\right)$

Chamfered groove rib Layek et al.[13]	Re : 3000 – 21,000 e/D : 0.022 – 0.04 p/e : 4.5 – 10 g/P : 0.3 – 0.6 Φ : 5 – 30 ^{o}	$Nu = 0.00225\ \mathrm{Re}^{0.92}\left(\frac{e}{D}\right)^{0.52}\left(\frac{p}{e}\right)^{1.72}\left(\frac{g}{p}\right)^{-1.21}\Phi^{1.24} \times\left[\exp\left\{-0.22(\ln\phi)^2\right\}\right]\left[\exp\left\{-0.46\left(\ln\frac{g}{p}\right)^2\right\}\right] \times\left[\exp\left\{-0.74\left(\ln\frac{g}{p}\right)^2\right\}\right]$	$f = 0.0024\,\mathrm{Re}^{-0.124}\left(\frac{e}{D}\right)^{0.365}\left(\frac{P}{e}\right)^{4.32}\left(\frac{g}{P}\right)^{-1.124} \times\exp[0.005\Phi]\exp\left[-1.09\left(\ln\frac{p}{e}\right)^2\right] \exp\left[-0.68\left(\ln\frac{g}{p}\right)^2\right]$
Arc shape rib Saini and Saini[16]	W/H :12 p/e :10 e/D : 0.0213 – 0.0422 $\alpha/90$: 0.3333 – 0.6666 Re : 2000 – 17,000	$Nu = 0.001047\mathrm{Re}^{1.3186}(e/D)^{0.3772}(\alpha/90)^{-0.1198}$	$f = 0.14408\ \mathrm{Re}^{-0.17103}(e/D)^{0.1765}(\alpha/90)^{0.1185}$
Dimple shape rib Saini and Verma [18]	Re : 2000 – 18,000 e/D = 0.0181 – 0.037 p/e = 8 – 12	$Nu = 5.2\times10^{-4}\ \mathrm{Re}^{1.27}\left(\frac{p}{e}\right)^{3.15} \times\left[\exp\left(-2.12\left(\log\left(\frac{p}{e}\right)\right)^2\right)\right]\left(\frac{e}{D}\right)^{0.033} \times\left[\exp\left(-1.30\left(\log\left(\frac{e}{D}\right)\right)^2\right)\right]$	$f = 0.642\ \mathrm{Re}^{-0.423}\left(\frac{p}{e}\right)^{-0.465} \left[\exp\left(0.054\left(\log\left(\frac{p}{e}\right)\right)^2\right)\right] \times\left(\frac{e}{D}\right)^{-0.0214}\left[\exp\left(0.840\left(\log\left(\frac{e}{D}\right)\right)^2\right)\right]$
Metal grit rib Karmare and Tikekar [22]	Re : 4000 – 17,000 e/D : 0.035 – 0.044 p/e : 12.5 – 36 l/s : 0.3 – 0.6	$Nu = 2.4\times10^{-3}\times(\mathrm{Re})^{1.3}\times(e/D)^{0.45} \times(l/s)^{-0.146}\times(p/e)^{-0.27}$	$f = 15.55\times(\mathrm{Re})^{-0.26}\times(e/D)^{0.91} \times(l/s)^{-0.27}\times(p/e)^{-0.51}$
Inclined-transverse rib Varun et al. [19]	Re : 2000 – 14,000 e/D : 0.030 p/e : 3 – 8	$Nu = 0.0006\ \mathrm{Re}^{1.213}(p/e)^{0.0104}$	$f = 1.0858\ \mathrm{Re}^{-0.3685}(p/e)^{0.0114}$
Multiple V-shape ribs Multiple V-ribs[26]	Re : 2000 – 20,000 e/D : 0.019 – 0.043 p/e : 6 – 12 W/w : 1 – 10 α : 30 ^{o} – 75 ^{o}	$Nu = 3.35\times10^{-5}\ \mathrm{Re}^{0.92} \times\left(\frac{e}{D}\right)^{0.77}\left(\frac{W}{w}\right)^{0.43}\left(\frac{\alpha}{90}\right)^{-0.49} \times\exp\left[-0.1177\,(Ln\,(W/w))^2\right] \times\exp\left[-0.61\,(Ln\,(\alpha/90))^2\right]\left(\frac{P}{e}\right)^{8.54} \times\exp\left[-2.0407\,(Ln\,(P/e))^2\right]$	$f = 4.47\times10^{-4}\ \mathrm{Re}^{-0.3188} \times\left(\frac{e}{D}\right)^{0.73}\left(\frac{W}{w}\right)^{0.22}\left(\frac{\alpha}{90}\right)^{-0.39} \times\exp\left[-0.52\,(Ln\,(\alpha/90))^2\right]\left(\frac{P}{e}\right)^{8.9} \times\exp\left[-2.133\,(Ln\,(P/e))^2\right]$

Transverse and inclined ribs

Varun *et al*. [19] carried out an experimental study on the heat transfer and fluid flow characteristics of the combine inclined and transverse wire rib of the absorber plate of a solar air heater duct as shown in Fig.26. The experiments encompassed on Reynolds number (Re) 2000 to 14000, relative roughness pitch (p/e) 3 to 8, and the relative Roughness height (e/D) 0.03.They reported the absorber plate with relative roughness pitch 8 gives maximum thermal efficiency.

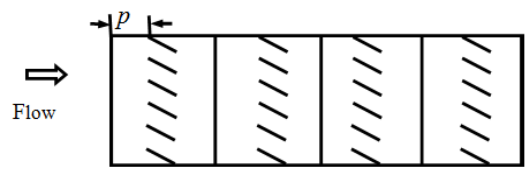

Fig. 26. combines inclined and transverse ribs [19]

Arc Shape ribs

Saini and Saini [16] investigated the heat transfer and fluid flow characteristics of arc shape roughness of a solar air heater duct as shown in Fig 18. The experiment encompassed on the parameters of duct aspect ratio (W/H) 12, relative roughness pitch (p/e) 10, relative roughness height (e/d) 0.0213-0.0422, relative angle of attack (α/90) 0.333-0.666 and Reynolds number for the range of 2000-17000.It has been observed that with the decrease in the arc angle there is a increase in heat transfer but with the increase in arc angle there is a decrease in friction factor. This is the advantages of arc shape roughness geometry. Author reported the maximum value of Nusselt number 3.80 times of smooth duct corresponding for the relative angle of arc (α/90) of 0.333 and for fixed roughness height (e/D) 0.0299.The friction factor 1.75 times of the smooth duct corresponding to same arc angle and relative roughness height 0.0422.

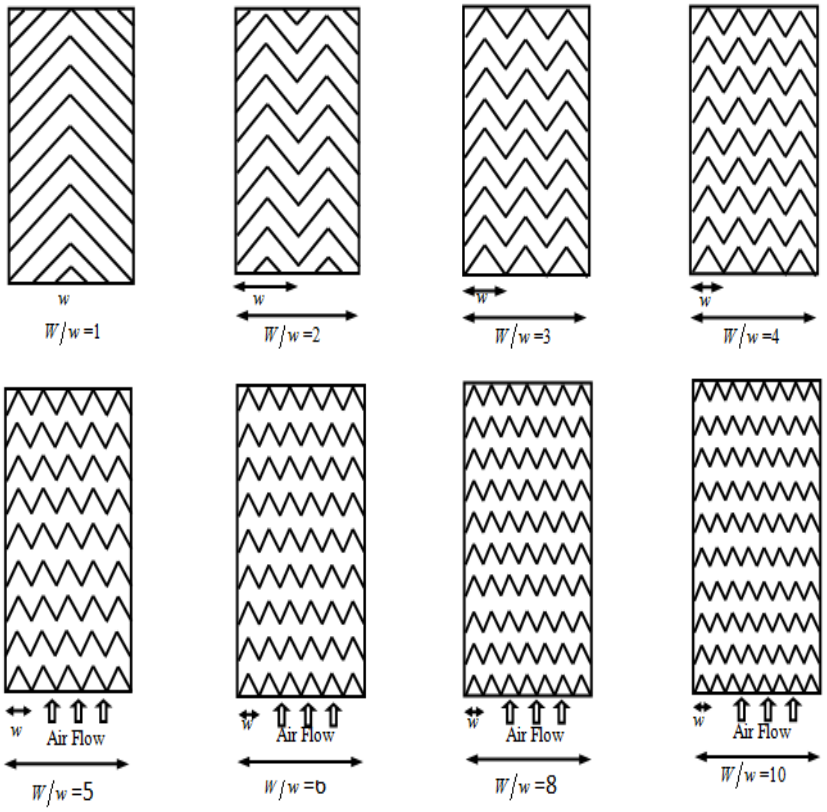

Fig. 27. Roughness geometry with metal grits [26]

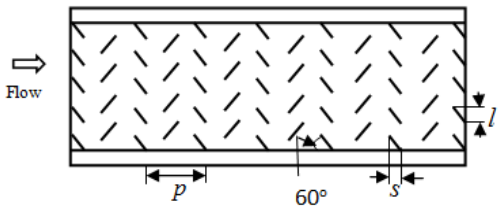

Fig. 28. Roughness geometry with metal grits [22]

Expanded metal mesh

Saini and Saini [17] investigated the effect of expanded metal mesh geometry on the heat transfer and fluid flow characteristics of a solar air heater ducts shown in Fig. 21. The range of parameter such as the relative long way of mesh (L/e) 25.00 -71.87 relative short way of mesh (S/e) 15.67-46.87 and the relative roughness height of the mesh (e/D) 0.012-0.0390, Reynolds number (Re) 1900-13000 and a large aspect ratio (W/H) 11:1 of the duct is selected. They reported the heat transfer and friction factor of order 4 and 5 times over the smooth duct corresponding to the angle of attack 61.2^o and 72^o respectively. The optimum thermohydraulic parameter is 2.34.

Inverted U-shape turbulators

There formed two stagnant eddies/circulation zones on the upstream and down side of transverse ribs. The formation of eddies not only reduce the heat transfer coefficient but also increases the pressure drop. With the opening the passage downstream the rib the intensity of eddies formation can be reduced. It has been found that in case of ribs formation of free shear layer depends on the number of sharp edges therefore in case of inverted U-shape ribs the two horizontal sharpen edges formed two shear layer on the downstream side which mixed up with accelerated flow and creates more turbulence on the reattachment point as shown in Fig.13. The side edges create secondary flow which also enhances heat transfer coefficient. Moreover the inverted U-shape turbulators operates on low Reynolds number where ribs are not applicable. Bopche and Tandale [15] studied the heat transfer and friction characteristics of inverted U-shape absorber plate as shown in Fig 13. The range of parameter selected were relative roughness height (e/D) 0.0186 to 0.03986 and turbulators pitch to height (p/e) ratio 6.67 to 57.14 were considered. The angle of attack of flow on the turbulators, α=90^o kept constant during the experiment. It has been observed that this turbulator geometry gives an appreciable heat transfer even at low Reynolds number where ribs are insufficient and as compared to the smooth duct; the turbulators roughened duct enhances the heat transfer and friction factor by 2.87 and 3.72 respectively.

Dimple Shape ribs

Dimple shape roughness is desirable due to low pressure drop and moderate heat transfer enhancement. The dimple shape roughness may be either protrusion or depression. The dimple shape roughness with depression induces flow separation and reattachment with pairs of vortices. The areas of high heat transfer include the areas of flow reattachment on the surface immediately downstream of the dimple. The heat transfer in the dimple surface with depression produces 2 to 2.5 times

greater than the heat transfer over smooth surface. The parameters that influence the heat transfer and fluid flow characteristics are channel height to dimple print diameter, dimple depth to dimple print diameter, longitudinal length of the absorber plate to dimple print diameter, span wise length of the absorber plate to the dimple print diameter. Moreover the dimple shape (cylindrical, hemispherical, teardrop) affect the heat transfer distribution in the solar air heater duct. Saini and Verma [18] studied experimentally the effect of protrusion dimple shape on the heat transfer and fluid flow characteristics in a solar air heater duct for the range of Reynolds number (Re) 2000 to 12000, relative roughness height (e/D) from 0.018 to 0.037 and relative roughness pitch (p/e) from 8 to 12 as shown in Fig 19. They reported the heat transfer is maximum corresponding relative roughness height (e/D) of 0.0379 and relative roughness pitch (p/e) of 10.The friction factor is minimum corresponding to relative roughness height (e/D) of 0.0289 and relative pitch (p/e) of 10.

Conclusion

In the present study, different type of roughness geometries has been presented by different investigators of solar air heater duct. The use of artificial roughness brings about a substantial improvement in the performance of the solar air heater duct resulting in size reduction or maximizing of heat transfer rate. Therefore a generation of new artificial roughness will definitely give a better performance of solar air heater in future.

REFERENCES

[1] Brij Bhusan, Ranjit Singh, A review on methodology of artificial roughness used in duct of solar air heaters: Energy 35(2010) 202-212.

[2] Frank k., Mark SB., Principles of heat transfer. Colorado: Thomson Learning Inc; 2001

[3] Webb RL, Eckert ERG. Heat transfer and friction in tubes with repeated-rib roughness. Int. J Heat Mass Transfer 1971; 14:601-17.

[4] Prasad BN, Saini JS. Effect of artificial roughness on heat transfer and friction factor in a solar air heater. Solar Energy 1988; 41(6):555-60.

[5] Verma SK, Prasad BN. Investigation for the optimal thermo hydraulic performance of artificially roughened solar air heaters. Renew Energy 2000; 20:19–36.

[6] Gupta D, Solanki S. C. and Saini J. S., Thermo-hydraulic performance of solar air heaters with roughened absorber plates. Solar Energy. Vol. 6, pp.33-42, 1997.

[7] Momin AME, Saini JS, Solanki SC. Heat transfer and friction in solar air heater duct with V-shaped rib roughness on absorber plate. Int J Heat Mass Transfer 2002; 45:3383–96.

[8] Sahu MM, Bhagoria JL. Augmentation of heat transfer coefficient by using 90^o broken transverse ribs on absorber plate of solar air heater. Renew Energy 2005; 30:2057–63.

[9] Muluwork KB, Saini JS, Solanki SC. Studies on discrete rib roughened solar air heaters. In: Proceedings of National Solar Energy Convention, Roorkee; 1998. pp. 75–84.

[10] Karwa R., Solanki S. C. and Saini J. S. Heat transfer coefficient and friction factor correlations for the transient flow regime in rib-roughened rectangular ducts. International Journal of heat and mass transfer. Vol. 42, pp 1597-1615, 1999

[11] Bhagoria J. L., Saini J. S. and Solanki S. C. Heat transfer coefficient and friction factor correlation for rectangular solar air heater duct having transverse wedge shaped rib roughness on absorber plate. Renewable Energy. Vol. 25, pp. 341-369, 2002.

[12] Jaurker A. R., Saini J. S. and Gandhi B. K. Heat transfer and friction characteristics of rectangular solar air heater duct using rib grooved artificial roughness. Solar Energy. Vol. 80, pp. 895–907, 2006.

[13] Layek A., Saini J. S. and Solanki S. C. Heat Transfer and Friction Characteristics for Artificially Roughened Ducts with Compound turbulators. International Journal of Heat and Mass Transfer. Vol. 50 pp. 4845–4854, 2007.

[14] Pawar CB, Aharwal KR, Chaube Alok Heat Transfer and fluid flow characteristics of rib-groove roughened solar air heater ducts. Indian Journal of Science and Technology 2009. Vol.2 No.11 pp. 50-54.

[15] Bopche SB, Tandale MS, Experimental Investigation on Heat Transfer and Friction Characteristics of a turbulators Roughened Solar Air Heater Duct. Int. Journal of Heat and Mass Transfer. Vol.52, pp. 2834-2848, 2009.

[16] Saini SK, Saini RP. Development of correlations for Nusselt number and friction factor for solar air heater with roughened duct having arc-shaped wire as artificial roughness. Sol Energy 2008; 82:1118–30.

[17] Saini RP, Saini JS. Heat transfer and friction factor correlations for artificially roughened ducts with expended metal mesh as roughness element. Int J Heat MassTransf1997; 40(4):973–86.

[18] Saini RP, Verma J. Heat transfer and friction factor correlations for a duct having dimple-shape artificial roughness for solar air heaters. Energy 2008; 33:1277–87.

[19] Varun, Saini RP, Singal SK. Investigation of thermal performance of solar air heater having roughness elements as a combination of inclined and transverse ribs on the absorber plate. Renew Energy 2008; 33:1398–405.

[20] Kumar A, Bhagoria JL, Sarviya RM, Heat Transfer and Friction Correlations for Artificially Roughened Solar Air Heater Duct with Discrete W-shape ribs. Energy Conversion and Management 2009; 50; 2106-2117.

[21] Lanjewar A.M. Bhagoria J.L., Sarviya R.M. Indian Journal of science and Technology 2010; Vol. 3 No.8 pp. 908-910.

[22] Karmare SV, Tikekar AN. Heat transfer and friction factor correlation for artificially roughened duct with metal grit ribs. Int J Heat Mass Transfer 2007; 50:4342–51.

[23] Lews MJ. Optimization the thermohydraulic performance of rough surface. Int. J Heat mass Transfer 1975; 18: 1243-8.

[24] Subramanian Karthik. Turbulent heat transfer in a trapezoidal channel with transverse and V-shaped ribs two opposite walls. M.S Dissertation 2005; Texas A&M University.

[25] Lanjewar A.M. Bhagoria J.L., Sarviya R.M. Experimental Thermal and Fluid Science xxx (2011) xxx-xxx.

[26] Hans V.S., Saini R. P. and Saini J. S. Heat transfer and friction correlations of solar air heater duct roughened artificially with multiple V-ribs. Solar Energy. 84(2011) 898–911.

[27] Gupta D, Solanki SC, Saini JS. Heat and fluid flow in rectangular solar air heater ducts having transverse ribs roughness on the absorber plate. Sol. Energy 1993; 51(I); 31-7.

[28] Bejan Adrian. Convection Heat Transfer. Wiley India (P) Ltd: New Delhi

[29] F. Williams, J. Watts. The development of rough surfaces with improved heat transfer performance and a study of mechanisms involved\ Proceedings of the 3th International Heat Transfer Conference\ Paris 2(FC 5.5) (1970) 1-11.

[30] Taslim ME, Li T, Kretcher DM. Experimental investigation on heat transfer and friction in channels roughened with angled, V-shaped and discrete ribs on two opposite walls. Trans. ASME J Turbo machinery 1996; 118: 20-8.

[31] Aharwal KR, Gandhi BK, Saini JS. Experimental investigation on heat transfer enhancement due to a gap in an inclined continuous rib arrangement in a rectangular duct of solar air heater. Renewable Energy 2008; 33:585-96.

****